M. A. Abdelmoneum, M. U. Demirci, and C. T.-C. Nguyen, "Stemless wine-glass-mode disk micromechanical resonators," *Proceedings*, 16th Int. IEEE Micro Electro Mechanical Systems Conf., Kyoto, Japan, Jan. 19.-23, 2003, pp. 698-701.

STEMLESS WINE-GLASS-MODE DISK MICROMECHANICAL RESONATORS

Mohamed A. Abdelmoneum, Jing Wang, Mustafa U. Demirci, and Clark T.-C. Nguyen

Center for Integrated Microsystems
Department of Electrical Engineering and Computer Science
University of Michigan
Ann Arbor, Michigan 48109-2122, U.S.A.

ABSTRACT

Polysilicon wine-glass mode micromechanical disk resonators using a stemless, non-intrusive suspension structure have been demonstrated in both vacuum and atmospheric pressure at frequencies around 73.4 MHz with *Q*'s as high as 98,000 in vacuum, and 8,600 in atmosphere—the highest ever reported *Q*'s at this frequency range and in these environments for any on-chip micro-scale resonator. The *Q* of 98,000 in vacuum for this wine-glass mode resonator is more than 10X higher than measured on radial contour mode counterparts, and more than 8X higher than exhibited by published free-free beams at 70 MHz.

I. INTRODUCTION

With frequencies poised to break the GHz barrier [1], vibrating micromechanical ("μmechanical") resonators are emerging as viable candidates for on-chip versions of the high-*Q* resonators used in wireless communication systems [2] for frequency generation and filtering. However, the use of such devices in present-day communication transceivers is so far still hindered by several remaining issues, including: (1) impedance values higher than normally exhibited by macroscopic devices; (2) the need for vacuum to attain high *Q*; and (3) *Q* values for stiff UHF devices, although higher than achievable by any other on-chip technology, still limited to under 10,000 by anchor-related loss mechanisms.

This work introduces a new vibrating disk resonator design that utilizes a wine-glass resonant mode together with a stemless, non-intrusive suspension structure to achieve frequencies in the range of 73.4 MHz with *Q*'s on the order of 98,000 in vacuum and 8,600 in atmosphere—the highest ever reported *Q*'s at this frequency range and in these environments for any on-chip micro-scale resonator. Although its frequency range is perhaps not as high as that for radial-contour mode designs [3] (since it requires more scaling for the same frequency), the sheer *Q* of this wine-glass mode disk offers several important practical advantages, including: (1) substantially smaller motional resistance, leading to smaller termination resistance values for micromechanical filters, thereby greatly simplifying impedance-matching issues between MEMS and macroscopic devices in communication transceivers [4]; (2) a lower dc-bias voltage requirement, which alleviates the need for charge pumping in practical systems; and (3) high *Q* even under atmospheric pressure, making this device suitable for a variety of applications without the need for expensive vacuum packaging.

II. DEVICE STRUCTURE AND OPERATION

Figure 1 presents the wine-glass mode shape for a solid disk as simulated by ANSYS. Unlike previously demonstrated radial contour mode disk resonators [3], which exhibit aerial dilation only, the wine glass vibration mode involves

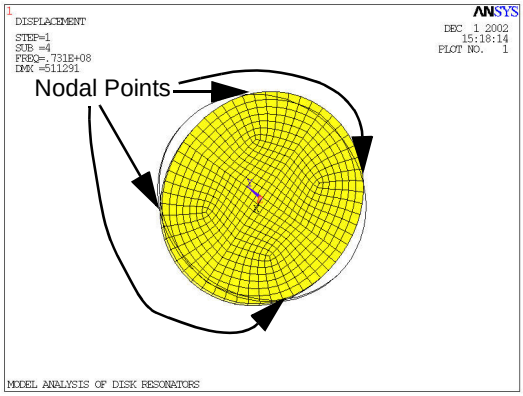

Fig. 1: Mode shape simulated by the finite element analysis package ANSYS.

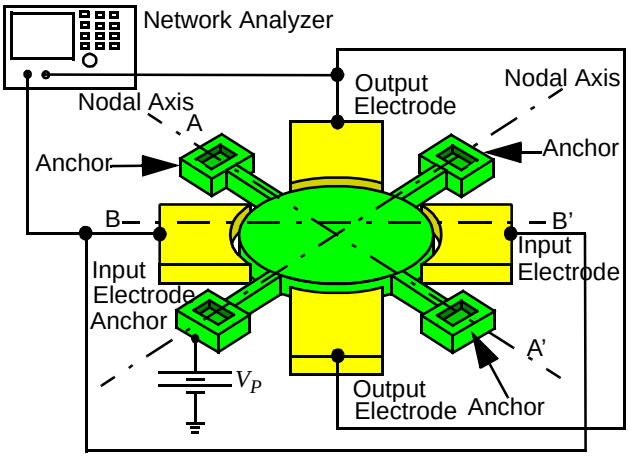

Fig. 2: Perspective-view schematic of the stemless wine-glass mode disk resonator in a typical two-port bias and excitation configuration.

both aerial dilation as well as rotation, yielding a compound mode shape with nodal axes that terminate at specific nodal points on the disk perimeter, and at the center of the disk. The existence of additional nodes in the wine-glass mode shape versus the radial mode shape allows for greater flexibility in anchoring this structure, hence, more opportunity for suppressing anchor-derived energy losses, allowing higher *Q*.

Figure 2 presents the perspective-view schematic of the wine-glass mode disk resonator used for this work in a typical bias and excitation configuration. This resonator features four anchored supports attached to the disk at its four wine-glass nodal points, and no stem anchor at its center. The lack of a stem allows this device to avoid anchor losses associated with misalignment of the stem and disk that plagued previous radial contour-mode disks. In particular, if the stem is not aligned exactly to the center of the disk, an inertial inbalance ensues that permits energy losses through the stem to the sub-

strate, hence, lowering the Q of the resonator. By trading a stem anchor for four perimeter supports with attachment locations defined in the same masking step as the structure itself (making misalignment impossible), this wine-glass resonator should be able to operate with substantially higher Q than radial mode counterparts. The stemless support structure also serves to single out the wine-glass mode of choice, while suppressing other unwanted modes—a very attractive feature for communication oscillator and filter applications.

Aside from the support structure, electrodes separated by only 1,000Å from the disk itself are placed around its circumference in each of the four quadrants for electrostatic excitation and detection. As shown in Fig. 2, to select the wine-glass mode shape, identical signals should be applied on opposing electrodes along one axis. The electrodes on the orthogonal axis can then either be directed to a sensing circuit; or connected to an out-of-phase input signal to add additional drive force.

III. DESIGN AND EQUIVALENT CIRCUIT

The dimensions needed to attain a specified resonance frequency f_o for a wine-glass mode disk can be obtained by solving the mode frequency equation, given by [5]

$$\left[\Psi_2\left(\frac{\zeta}{\xi}\right) - 2 - q\right][2\Psi_2(\zeta) - 2 - q] = (nq - n)^2 \qquad (1)$$

where

$$q = \frac{\zeta^2}{2n^2 - 2}\ ,\ \zeta = R\sqrt{\frac{2\rho\omega_o^2(1+\sigma)}{E}}\ ,\ \xi = \sqrt{\frac{2}{1-\sigma}}\ , \qquad (2)$$

and where R is the disk radius, $\omega_o = 2\pi f_o$ is the angular frequency, n is the mode, and ρ, σ, and E are the density, Poisson ratio, and Young's modulus, respectively, of the disk structural material.

As with other vibrating resonators, the equivalent LCR circuit for the wine-glass disk is governed by the total integrated kinetic energy in the resonator, its mode shape, and parameters associated with its transducer ports [4]. Using the procedure of [4], the expressions for equivalent inductance L_x, capacitance C_x, and resistance R_x can be written as

$$L_x = \frac{m_{re}}{\eta_e^2} \qquad C_x = \frac{\eta_e^2}{\omega_o^2 m_{re}} \qquad R_x = \frac{\omega_o}{Q}\frac{m_{re}}{\eta_e^2} \qquad (3)$$

where

$$m_{re} = \frac{\rho\pi h \int_0^R \left[\frac{G}{2r}J_1(G) - \frac{G}{2r}J_3(G) + \frac{2B}{RA}J_2(G\xi)\right]^2 r\,dr}{\left[\frac{G}{2r}J_1\left(\frac{\zeta}{\xi}\right) - \frac{G}{2r}J_3\left(\frac{\zeta}{\xi}\right) + \frac{2B}{RA}J_2(\zeta)\right]^2}\ , \qquad (4)$$

$$G = \frac{\zeta r}{\xi R}\ ,\ \eta_e = V_P\left(\frac{\partial C}{\partial x}\right)\ , \qquad (5)$$

h is thickness, $B/A = -4.5236$, and $(\partial C/\partial x)$ is the integrated change in electrode-resonator capacitance per unit displacement for a single quadrant port in Fig. 2.

One important difference between the stiff, high frequency resonators of this work and previous lower frequency ones is the difference in total energy per cycle. In particular, the peak kinetic energy per cycle can be computed via the expression

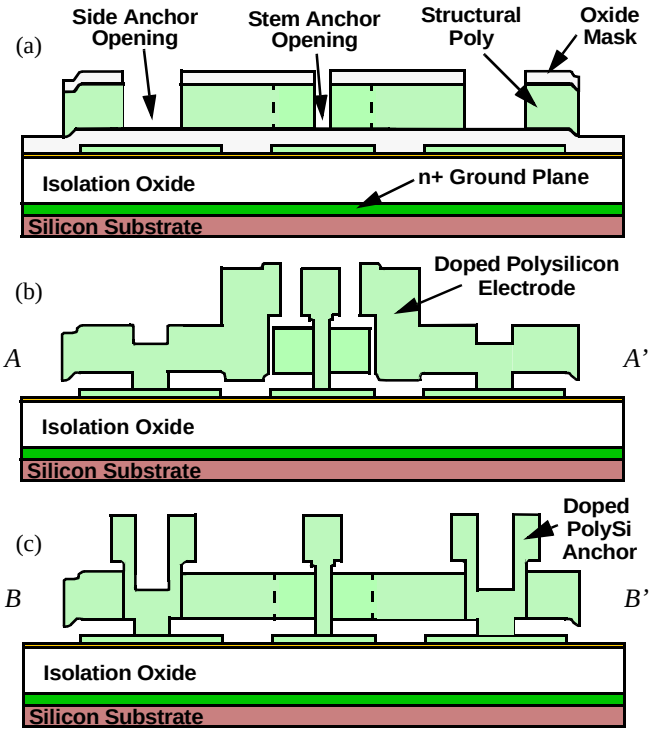

Fig. 3: Fabrication cross-sectional process flow for the devices of this work. (a) Cross-section showing the stem and side anchor vias after the structural polysilicon etch step. (b) Cross-section along AA' of Fig. 2 of a finished disk resonator, showing the overhanging polysilicon electrodes. (c) Cross-section along BB' of Fig. 2, showing the center and side supports after release.

$$KE_{peak} = \frac{1}{2}m_{re}(\omega_o X)^2 = \frac{1}{2}k_{re}X^2\ , \qquad (6)$$

where X and k_{re} are the peak displacement and effective stiffness, respectively, at the disk location across from the center of an electrode. Given that the k_{re} ~542,000 N/m for a 73-MHz wine-glass resonator is more than 350X the 1,500 N/m of a 10-MHz CC-beam, the former is expected to store 350X more energy per cycle for the same displacement amplitude. With energies per cycle many times larger than those lost to viscous gas damping, the wine-glass resonators of this work, and virtually any high stiffness, high frequency μmechanical resonator device (e.g., radial contour mode disks), are expected to exhibit high Q even under air damped conditions.

IV. FABRICATION PROCESS

With the intention of circumventing structural rigidity problems associated with plated metal electrodes in previous radial-contour mode disk resonators [3], the fabrication process used in this work differs from previous ones in that polysilicon electrodes are used instead of metal.

Figure 3 presents cross-sections summarizing the process flow. The process begins with polysilicon surface micromachining steps similar to those used in a previous metal electrode small-gap process [6] up to the point of defining the disk structure. The process then deviates from [6] with an etch step that patterns not only the disk and support structures, but also vias for any anchors to be formed, yielding the cross-section shown in Fig. 3(a). A sidewall sacrificial oxide spacer is then deposited to define the electrode-to-resonator gap, as in [6], but additional steps are taken to remove this

Table I: Wine-Glass Disk Design and Performance Summary

Parameter	With Stem 4-pts.	Stemless 4-pts.	Stemless 2.5-pts.	Stemless 2-pts.	Units
μDisk Dimensions: R, h	26.5, 1.5	26.5, 1.5	26.5, 1.5	26.5, 1.5	μm
Electrode-to-Resonator Gap, d_o	1,000	1,000	1,000	1,000	Å
DC-Bias Voltage, V_P	5	7	7	7	V
Meas. Resonance Frequency, f_o	73.66	73.422	73.432	73.615	MHz
Quality Factor in Vacuum, Q	3,683	11,748	57,594	98,000	—
Quality Factor in Air, Q	2,427	5,439	7,000	8,600	—
Meas. Motional Resistance, R_x	174.19	113.15	33	13.23	kΩ

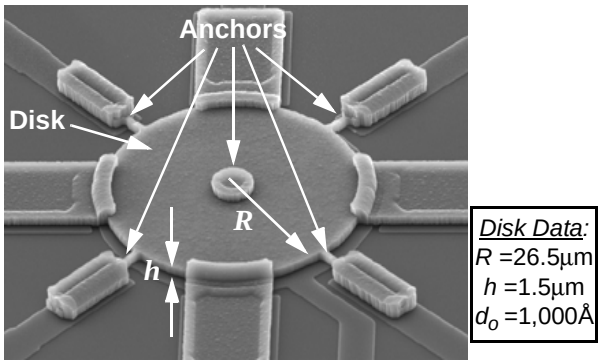

Fig. 4: SEM of a 73-MHz wine-glass mode resonator with stem and four perimeter nodal supports.

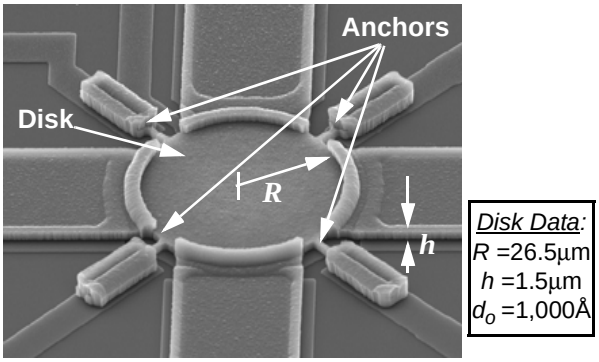

Fig. 5: SEM of a 73-MHz stemless wine-glass mode resonator with four perimeter nodal supports

sidewall sacrificial layer in the anchor vias, then etch through the bottom-side sacrificial layer down to the substrate. With exposed anchor vias, a subsequent (third) polysilicon deposition then not only provides the material for electrodes, but also refills the anchor vias to create very rigid, self-aligned anchors. This third polysilicon layer is then $POCl_3$-doped and patterned to delineate the electrodes.

After an HF release etch, the remaining cross-sections, taken along the axes indicated in Fig. 2, are as shown in Figs. 3(b) and (c).

V. EXPERIMENTAL RESULTS

Wine-glass mode disk resonators with resonance frequencies around 73 MHz were designed and fabricated using the above polysilicon-electrode process. For comparative purposes, each device design was implemented with two support variations: (1) both stem and perimeter nodal supports; and (2) perimeter nodal supports only. Table I summarizes each design. Figures 4 and 5 present the scanning electron micrographs (SEM's) for 73-MHz versions with four perimeter nodal anchors, with and without the stem, respectively.

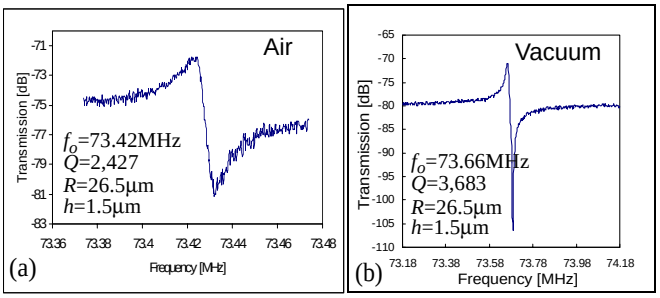

Fig. 6: Measured frequency spectra in (a) air and (b) vacuum for a 73-MHz wine-glass mode resonator with stem and four perimeter nodal supports.

Devices were tested using a custom-built vacuum chamber capable of achieving pressures down to 50 μTorr, and equipped with feedthroughs to allow electrical connections between external instrumentation and the board-mounted resonator die within. The direct two-port measurement circuit shown in Fig. 2 was used to make all measurements to follow. Note that no provisions were made to impedance-match the resonators under test to the 50Ω network analyzer input, so it should be understood that losses seen in the transmission measurements to follow are caused by impedance-mismatching, and are not indicative of device loss. By their sheer high Q, it should be obvious that the devices will have very little loss when used in properly matched filters [4].

Wine-glass mode resonators with both stem and perimeter nodal supports were tested first. Figure 6 presents the measured frequency spectrum for a 73-MHz version measured in (a) air and (b) vacuum, using the circuit of Fig. 2. As shown, this device exhibits a Q of 3,600 in vacuum, and a Q of 2,400 in air, the latter verifying the prediction of Section III that these high stiffness, high frequency resonators should still exhibit high Q even under atmospheric pressure.

Stemless 73-MHz devices with four perimeter nodal supports were then tested, yielding the measured frequency spectra shown in Fig. 7 with Q's of 5,439 and 11,748 in air and vacuum, respectively. Thus, removal of the center stem anchor results in an increase of the attainable Q (in vacuum) by a factor of 4X for this wine-glass mode resonator. This clearly supports a model where the stem anchor, with its potential for misalignment, dominates energy losses for disk resonators in vacuum.

Further insight into the effect of anchors on wine-glass mode resonator Q was obtained through a fortuitous deficiency in this particular process run that yielded a limited set

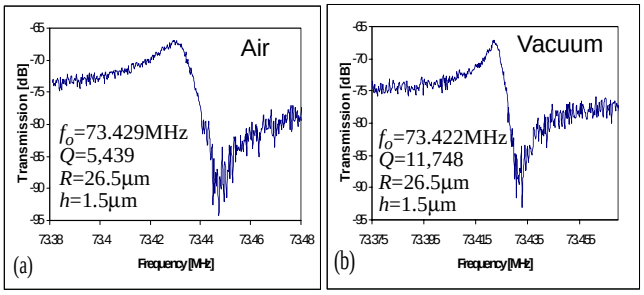

Fig. 7: Measured frequency spectra in (a) air and (b) vacuum for a 73-MHz stemless wine-glass mode resonator with four perimeter nodal supports.

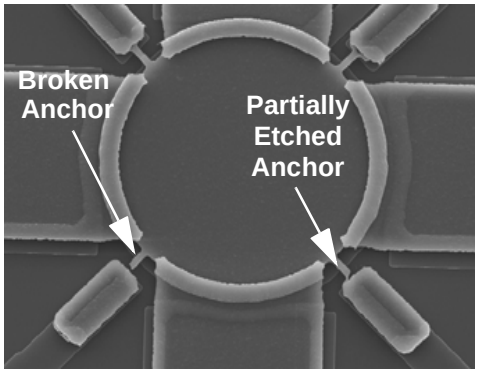

Fig. 8: Top-view SEM of a 73-MHz stemless wine-glass mode disk with broken perimeter supports.

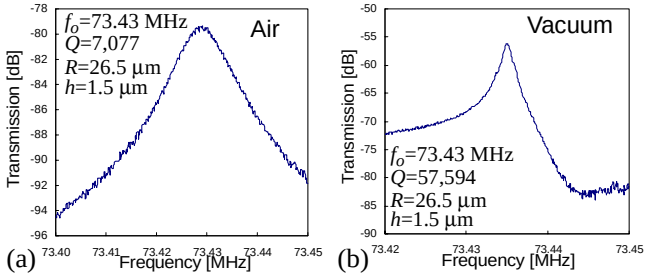

Fig. 9: Measured frequency spectra in (a) air and (b) vacuum for a 73-MHz stemless wine-glass mode resonator with 2.5 perimeter nodal supports.

of stemless devices with broken perimeter nodal supports. In particular, Fig. 8 presents the top-view SEM of one such device, where one of the four perimeter supports is cleanly broken off, and another is partially broken, leaving a device supported by roughly two and a half perimeter anchors. The measured frequency spectra in air and vacuum for this device are shown in Fig. 9, where an exceptional Q in vacuum of 57,594 is seen, which is more than 5X that of previously measured micromechanical disk resonators. The fact that this performance was attained by decreasing further the number of supports further attests to a model where anchor losses dominate the Q in vacuum. Note also the Q of 7,007 that this device exhibits in air, continuing the high Q trend seen repeatedly for these devices at atmospheric pressure.

Finally, Fig. 10 presents the measured frequency spectrum for a stemless 73-MHz wine-glass disk with only two perimeter nodal supports, located in the upper half of the disk. With yet fewer supports, the Q in vacuum for this resonator is even higher, at about 98,000, further supporting a mechanism where Q is governed by anchor losses. The fact that this

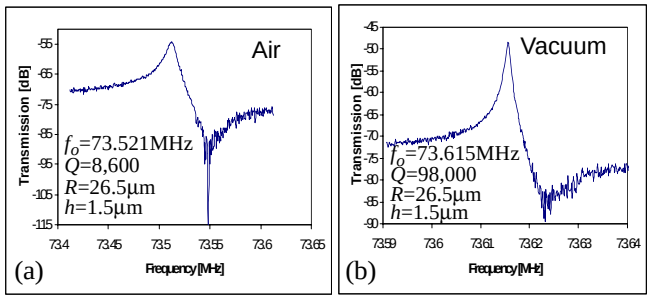

Fig. 10: Measured frequency characteristic in (a) air and (b) vacuum for a 73-MHz stemless wine-glass mode resonator with 2 perimeter nodal supports.

value of Q is among the highest measured in polysilicon devices at any frequency, low or high, suggests that contributions from internal material loss mechanisms are not necessarily increasing with frequency, at least not up to 73 MHz.

With high Q's in both air and vacuum, the device of Fig. 10 also achieves small values of series motional resistance R_x: 2.7 kΩ in vacuum with V_P=16V, and 26 kΩ in air with V_P=28V. Table I provides a concise summary of other relevant performance parameters for each tested resonator.

VI. CONCLUSIONS

By eliminating anchor-to-disk misalignment error (by removing the stem) and minimizing the number perimeter nodal supports, the wine-glass mode polysilicon micromechanical disk resonators of this work have now achieved a frequency-Q product of 7.2×10^{12}—the highest to date for polysilicon resonator devices. Even with the conservative assumption that Q might roll off linearly with frequency, this f_o-Q product suggests that the Q's of 7,200 at 1 GHz are not unreasonable. Furthermore, when operated and measured in air, the stemless, 2-support device of Fig. 10 exhibits a Q of 8,600, which is the highest ever reported for a polysilicon μmechanical resonator operating at atmospheric pressure. The implications here are enormous, as this result effectively states that vacuum is no longer needed to attain exceptional Q in high frequency vibrating micromechanical resonators—a fact that should substantially lower the cost of devices based on vibrating RF MEMS technology, making them strong contenders in many communications applications.

Acknowledgment. This work was supported by DARPA and an NSF ERC in Wireless Integrated Microsystems.

References.

[1]C. T.-C. Nguyen, "Vibrating RF MEMS for Low Power Communications," to be published in the *Proceedings* of the 2002 Fall MRS Meeting, Boston, MA, Dec. 2-6.

[2]C. T.-C. Nguyen, *Dig. of Papers*, Topical Mtg on Silicon Monolithic IC's in RF Systems, Sept. 12-14, 2001, pp. 23-32.

[3]J. R. Clark, W.-T. Hsu, and C. T.-C. Nguyen, *Technical Digest*, IEEE Int. Electron Devices Meeting, San Francisco, California, Dec. 11-13, 2000, pp. 399-402.

[4]F. D. Bannon III, J. R. Clark, and C. T.-C. Nguyen, *IEEE J. Solid-State Circuits*, vol. 35, no. 4, pp. 512-526, April 2000.

[5]M. Onoe, "Contour vibrations of isotropic circular plates", *J. of Acoustical Society of America*, vol. 28, no.6, pp. 1158-11662, Nov. 1954.

[6]W.-T. Hsu, J. R. Clark, and C. T.-C. Nguyen, *Technical Digest*, 14th Int. IEEE MEMS Conference, Interlaken, Switzerland, Jan. 21-25, 2001, pp. 349-352.